Helix Packing in the Lactose Permease of *Escherichia coli*: Distances between Site-Directed Nitroxides and a Lanthanide†

John Voss,‡ Jianhua Wu,§,|| Wayne L. Hubbell,⊥ Vincent Jacques,‡ Claude F. Meares,‡ and H. Ronald Kaback*,§

Howard Hughes Medical Institute, Departments of Physiology and of Microbiology & Molecular Genetics, and Jules Stein Eye Institute and Department of Chemistry and Biochemistry, University of California, Los Angeles, California 90095, and Chemistry Department, University of California, Davis, California 95616-0935

Received October 5, 2000; Revised Manuscript Received January 4, 2001

ABSTRACT: By exploiting substrate protection of Cys148 in lactose permease, a methanethiosulfonate nitroxide spin-label was directed specifically to one of two Cys residues in a double-Cys mutant, followed by labeling of Cys148 with a thiol-reactive chelator that binds Gd(III) quantitatively. Distances between bound Gd(III) and the nitroxide spin-label were then studied by electron paramagnetic resonance. The results demonstrate that the Gd(III)-induced relaxation effects on nitroxides at positions 228, 226 (helix VII), and 275 (helix VIII) agree qualitatively with results obtained by studying spin−spin interactions [Wu, J., Voss, J., et al. (1996) *Proc. Natl. Acad. Sci. U.S.A. 93*, 10123−10127]. Thus, a nitroxide attached to position 228 (helix VII) is closest to the lanthanide at position 148 (helix V), a nitroxide at position 275 (helix VIII) is further away, and the distance between positions 226 (helix VII) and 148 is too long to measure. However, the Gd(III)−spin-label distances are significantly longer than those estimated from nitroxide−nitroxide interactions between the same pairs due to the nature of the chelator. Although the results provide strong confirmation for the contention that helix V lies close to both helices VII and VIII in the tertiary structure of lactose permease, other methods for binding rare earth metals are discussed which do not involve the use of bulky chelators with long linkers.

Double-labeling techniques are useful for spectroscopic studies of protein structure and dynamics (*1*, *2*). However, a major limitation of the approach is the difficulty inherent in directing probes to specific sites in a given protein. However, development of site-specific mutagenesis has largely allowed this problem to be overcome (see *3*, *4*).

Substrate protection of Cys148 against alkylation is a well-characterized property of lactose permease (lac permease)[1] (*5*−*8*). In the presence of saturating concentrations of β,D-galactopyranosyl 1-thio-β,D-galactopyranoside (TDG), the reactivity of Cys148 with various alkylating agents is completely blocked. Therefore, it is possible to exploit this property of the permease by constructing mutants containing two Cys residues, one native Cys at position 148 that can be protected in the presence of TDG and another at a different position that is labeled covalently with a given alkylating agent in the presence of the analogue. Subsequently, after removal of TDG, Cys148 can be labeled with a different alkylating agent. By using this approach and alkylating agents with appropriate spectroscopic properties, distances between position 148 and other positions in the protein can be measured.

Site-directed spin-labeling (SDSL)[1] is a powerful spectroscopic approach for structure/function studies (*9*). By this means, a spin-labeled side chain is introduced at specific sites by Cys-substitution mutagenesis (*10*), and electron paramagnetic resonance (EPR) spectra are analyzed in terms of side chain dynamics, solvent accessibility, polarity, and electrostatic potential. Information of this type from a set of spin-labeled mutants can be used to determine protein topography (*11*−*16*), secondary structure (*14*, *16*−*18*), and certain features of tertiary organization (*18*, *19*).

SDSL also provides a method to measure distance when a second paramagnetic center is present. Introduction of two nitroxides into a protein and analysis of static dipolar interaction is one approach that has been exploited (*2*, *20*−*23*). In this case, rotational diffusion of the spin pair may complicate interpretation of the interaction, a restriction that often requires freezing of the sample. In addition to the problem of possible structural changes, freezing eliminates the possibility of studying dynamics. Here we utilize another approach based on the magnetic interaction between a spin-label and a paramagnetic metal ion which is applicable under

† This work was supported in part by NIH Grant DK 51131 to H.R.K. and NIH Grant EY05216 to W.L.H., as well as by the Jules Stein Professor endowment.

* To whom correspondence is to be addressed. Tel: (310)206-5053; Fax: (310)206-8623; E-mail: RonaldK@HHMI.UCLA.edu.

‡ Chemistry Department, University of California, Davis.

§ Howard Hughes Medical Institute, Departments of Physiology and of Microbiology & Molecular Genetics, University of California, Los Angeles.

|| Present address: Genome Therapeutics Corp., Waltham, MD 02453-8443.

⊥ Jules Stein Eye Institute and Department of Chemistry and Biochemistry, University of California, Los Angeles.

[1] Abbreviations: lac permease, lactose permease; TDG, β,D-galactopyranosyl 1-thio-β,D-galactopyranoside; EPR, electron paramagnetic resonance; methanethiosulfonate spin-label, (1-oxyl-2,2,5,5-tetramethylpyrroline-3-methyl)methanethiosulfonate; C-less permease, functional lactose permease devoid of native Cys residues; SDSL, site-directed spin-labeling; KP_i, poassium phosphate; Gd(III)−BAD, 6-[*p*-(bromoacetamido)benzyl]-1,4,7,10-tetraazacyclododecane-*N*,*N*′,*N*″,*N*‴-tetraacetic acid with bound Gd(III).

10.1021/bi002333e CCC: $20.00
Published on Web 02/15/2001

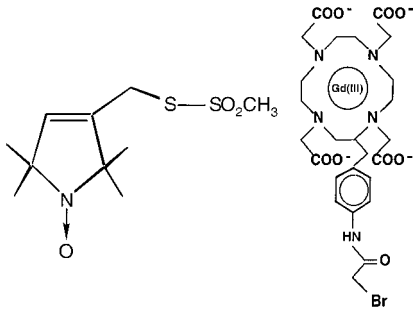

A **B**

FIGURE 1: (A) Structure of the spin-labeled side chain R1. (B) Structure of thiol-reactive Gd(III)−BAD.

physiological conditions.

Previously (*24*−*26*), the distance-dependent relaxation effect of Cu(II) on a nitroxide was analyzed according to the paradigm of Leigh (*27*). In this communication, the effect of Gd(III) sequestered by a chelator bound covalently to Cys148 on spin-labeled side chains at positions 226, 228, or 275 is investigated. Gd(III) has a larger magnetic moment than Cu(II), for example, and is ideally suited for Leigh analysis, since longer interspin distances can be probed. The results obtained are in good qualitative agreement with previous studies utilizing site-directed chemical cleavage (*28*), spin−spin interactions, and chemical cross-linking (*21*). On the other hand, distances estimated from Gd(III)−spin-label measurements are significantly overestimated relative to those derived from either spin−spin interaction or thiol cross-linking (*21*, *29*) due to use of a bulky chelator with a long linker. Alternative approaches are discussed.

EXPERIMENTAL PROCEDURES

Materials. (1-Oxyl-2,2,5,5-tetramethylpyrroline-3-methyl)-methanethiosulfonate (methanethiosulfonate spin-label) was a gift from Kálmán Hideg, and is available from Reanal (Budapest, Hungary). 6-[*p*-(Bromoacetamido)benzyl]-1,4,7,10-tetraazacyclododecane-*N*,*N*′,*N*′,*N*‴-tetraacetic acid complexed with a Gd(III) ion [Gd(III)−BAD] was synthesized as described previously (*30*, *31*).

Construction, Expression, and Purification of Mutant Permeases. Permease mutants containing given Cys replacements in the Cys-less background and a biotin acceptor domain in the middle cytoplasmic loop were prepared and purified by avidin affinity chromatography as described (*21*).

Labeling. *n*-Dodecyl-*β*,D-maltopyranoside (DDM)-solubilized permease containing native Cys148, another Cys residue at a given position, and the biotin acceptor domain in the middle cytoplasmic loop was bound to an immobilized monomeric avidin column (*21*) and equilibrated with 100 mL of column buffer [50 mM potassium phosphate (KP_i; pH 7.5)/100 mM KCl/0.02% DDM] containing 20 mM TDG in order to protect Cys148. The permease was then labeled with the methanethiosulfonate spin-label (100 μM, final concentration) at position 226, 228, or 275 (Figure 1A). Following 30 min incubation with the spin-label, the sample was washed with 400 mL of column buffer containing 20 mM TDG to remove unreacted methanethiosulfonate spin-label. TDG was then removed by an additional wash of 300 mL of column buffer. Following elution of the permease in 6 mL of column buffer containing 10 mM biotin, the mutant permease was concentrated to 100 mL using a Pro-Dicon concentrator (Spectrum) as described previously (*14*) and separated into two equal fractions. In one fraction [+Gd(III)], Cys148 was labeled with 0.5 mM Gd(III)−BAD (Figure 1B) for 2 h; in the control fraction, Cys148 was labeled with 0.5 mM *N*-iodoacetyltyrosine for 2 h (*6*). Finally, unreacted Gd(III)−BAD or *N*-iodoacetyltyrosine was removed from the sample by dialysis against column buffer using a Microdialysis Cell (Rainin Instrument Co.). It is noteworthy that the K_D of the chelator for Gd(III) approximates 10^{-24} M (*32*). Thus, it is unlikely that significant amounts of Gd(III) dissociate from covalently bound Gd(III)−BAD during the course of the experiments.

Protein Determinations. Protein was determined using the Micro BCA protein assay kit (Pierce Chemicals).

EPR Spectroscopy. EPR measurements on given spin-labeled permease mutants were performed in a quartz capillary at 22 °C. Ten microliters of sample containing purified permease at a final concentration of ca. 100 μM in 10 mM MES (pH 7.5)/0.02% DDM was used in each measurement. Spectra were signal-averaged over 10 scans using a Varian E-104 X-band spectrometer fitted with a loop−gap resonator (*33*, *34*) at a microwave power of 2 mW and a modulation amplitude of 2 G. The spectral intensity (I) was obtained from the peak-to-peak height of the center ($m_I = 0$) line and the low-field ($m_I = +1$) line of the spectrum.

Data Analysis. Spectral broadening due to dipolar interaction between a paramagnetic metal ion and a nitroxide as described by Leigh (*27*) was examined previously (*24*, *25*). Briefly, the treatment applies Redfield theory to describe the effect of the magnetic field (H_z), fluctuating with a correlation time of τ, from one spin on the line width (δH) of a second spin:

$$\delta H = \frac{g\beta\tau H_z}{\hbar} + \delta H_0 \tag{1}$$

with

$$H_z = \frac{\mu(1 - 3\cos^2\theta'_R)}{r^3} \tag{2}$$

where g is the electronic g factor of the nitroxide, β is the Bohr magneton, μ is the magnetic moment of the metal, and r is the interspin distance. The angular-dependent line width of the relaxed spin is simplified to

$$\delta H = C(1 - 3\cos^2\theta'_R)^2 + \delta H_0 \tag{3}$$

where C, the dipolar broadening coefficient, is

$$C = \frac{g\beta\mu^2\tau}{\hbar r^6} \tag{4}$$

For the $S = 7/2$ Gd(III) ion, a value of $8.0 \times \beta$ (*35*) was used to calculate μ. Leigh treatment assumes that τ is equal to T_{1e}, the electronic relaxation time of the metal (*24*). In the present work, complexed Gd(III) with a T_{1e} of 5.3×10^{-10} s at room temperature is employed (*36*).

A convenient feature of the theory is that the relaxed spins broaden to such an extent that they no longer contribute

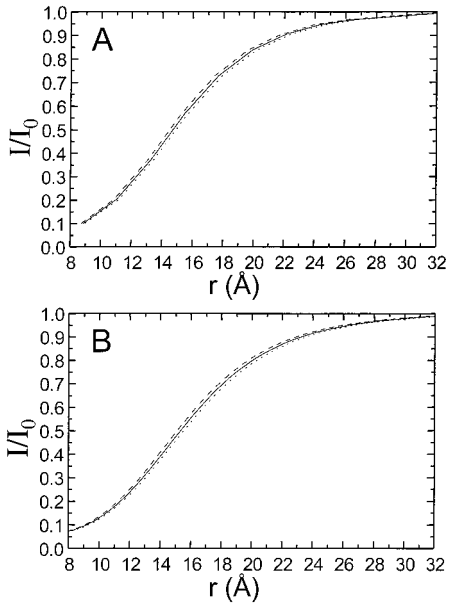

FIGURE 2: Plot of the interspin distance *r* versus the spectral amplitude (I/I_0) for the line widths of the spectra investigated: I275R1 (dashed line), Y228R1 (solid line), S226R1 (dotted line). The curves were generated from simulated broadening of either anisotropic (A) or isotopic (B) lines (see Experimental Procedures).

significantly to the observed spectral amplitude. The number of relaxed spins is distance-dependent, allowing for the determination of *r* by evaluating the loss in nitroxide spectral intensity (*I*) due to the broadening influence of a second paramagnetic center [in this case a Gd(III) ion].

The broadening is evaluated from a Lorentzian line shape function:

$$L = \frac{\delta H}{(H - H_m)^2 + \delta H^2} \quad (5)$$

Computer simulations of both isotropic and anisotropic lines for values of δH arising from different values of *C* were performed to generate a plot of the broadened amplitude to the unbroadened amplitude, I/I_0 vs $C/\delta H_o$, where δH_o is the line width in the absence of broadening induced by the metal (*24*). From this plot, the experimental I/I_0 value is used to obtain a value for *C*, and the interspin distance, *r*, is calculated from eq 4. Figure 2 shows the simulated spectral amplitude for values of *r* calculated, using a Gd(III) relaxer, for the natural line widths of the spectra examined in this study.

RESULTS

Spectra of S226R1/Cys148, Y228R1/Cys148, or I275R1/Cys148 Mutants with N-Iodoacetyltyrosine-Labeled Cys148. Spectra of control samples in which a Cys residue at position 226, 228, or 275 was labeled with nitroxide spin-label and Cys148 was labeled with iodoacetyltyrosine are shown in Figure 3 (thick line). Each spectrum is typical of a spin-labeled side chain within a stable transmembrane α-helix, as indicated by a significant low-field immobilized component (*14*, *18*, *37*). The peak-to-peak amplitude (*I*) of the center ($m_I = 0$) spectral line is indicated. The samples display a small highly mobile component (arrows), most likely arising from the presence of unreacted spin-label partitioned into the protein/micelle complex. To ensure that the intensity measured arises solely from label covalently attached to position 226, 228, or 275, the amplitude of the strongly immobilized component which is fully resolved in the low-field line ($m_I = +1$) was also measured (Figure 3; see below).

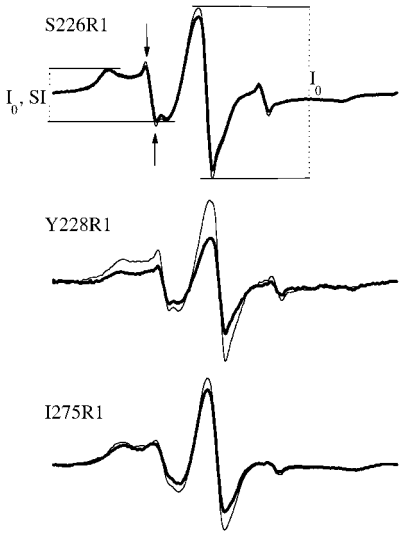

FIGURE 3: EPR spectra of S226R1, Y228R1, and I275R1 in combination with Cys148 reacted with either iodoacetamidotyrosine (thin line) or Gd(III)−BAD (thick line). The unbroadend spectral intensity (I_0) is indicated for the center ($m_I = 0$) line as well as for the strongly immobilized component resolved in the low field ($m_I = 0$) (I_0, SI).

Table 1: Spectral Parameters and Calculated Distances between Nitroxide-Labeled Cys Residues and the Gd(III)−Chelate at Cys148

R1 position	I/I_0[a]	δH_0 [b]	C[c]	*r*-calcd (Å)[d]
226	0.90	4.1	0.43−0.29	22.2−23.7
228	0.59	4.4	3.28−2.53	15.8−16.5
275	0.84	4.8	0.87−0.65	19.7−20.7

[a] The center spectral ($m_I = 0$) above-baseline amplitudes normalized to the metal-free control. [b] The natural line width, δH_0 (G), was obtained from the peak-to-peak width of the ($m_I = 0$). [c] The dipolar broadening coefficient obtained from the values of I/I_0 and δH_0 (see Experimental Procedures). [d] Calculated interspin distance using eq 4 under Experimental Procedures. The range of values reported for footnotes *c* and *d* reflects a *C* value obtained from the predicted broadening of either an anisotropic or an isotropic line (*24*, *25*). The difference in the interspin distance resulting from utilization of either an anisotropic or an isotropic simulation of the dipolar broadening is illustrated in Figure 2.

Effect of Bound Gd(III) on Spin-Labeled Permeases. EPR spectra for the three mutants with nitroxide spin-label at position 226, 228, or 275 and Gd(III)−BAD covalently attached to Cys148 are also shown in Figure 3 (thin line). The presence of Gd(III) reduces the spectral line height in each of the three mutants as a result of broadening. Ignoring the intrinsic line width dependency on the extent of broadening (see below), it is evident that Gd(III) reduces the spectral amplitude of Y228R1 the most, the spectral amplitude of S226R1 the least, and the spectral amplitude of I275R1 to an intermediate degree. The residual amplitude (I/I_0), the amplitude of the Gd(III)-broadened spectrum normalized to the amplitude of the control sample, is given in Table 1 for each of the three mutants measured.

Calculation of the Distance between the Gd(III) Ion and the Nitroxyl Moiety of the Labels at Position 226, 228, or 275. It was demonstrated previously (*25*) that the dipolar

broadening induced by a paramagnetic metal on a nitroxide attached to a protein can be analyzed as a function of distance by using the paradigm of Leigh (*27*). The strength of the dipolar broadening interaction is expressed in terms of *C*, the dipolar broadening coefficient. For a given unbroadened line width (δH_0), plotting *C* versus I/I_0 shows the predicted loss in peak height intensity (*14*) from which the distance between the paramagnetic metal and the spin-label can be approximated (Figure 2; Table 1). Consistent with the results of Wu et al. (*21*), positions 228 and 275 are closer to position 148 than position 226, which is thought to be on the opposite side of helix VII from position 228, and position 228 is closer than position 275.

The I/I_0 amplitudes listed in Table 1 are from the center ($m_I = 0$) line of the spectra. As noted above, the spectra exhibit a small but significant population of weakly immobilized spins whose contribution to the center ($m_I = 0$) line intensity is difficult to resolve. Therefore, the low-field line (Figure 3; $m_I = +1$), where the strongly immobilized signal representing covalently attached spin-label is clearly resolved, was also used to measure I/I_0 in each spectrum. The amplitudes determined in this manner are effectively identical to the center line ($m_I = 0$) amplitudes given in Table 1.

DISCUSSION

SDSL has recently been employed to investigate structure/function relationships in lac permease (*14*−*16*, *21*−*23*, *25*, *26*, *29*). Here, we present SDSL of three residues in the permease in combination with a Gd(III)−chelator attached specifically to Cys148. The broadening of nitroxides at positions 226, 228, and 275 due to a dipolar interaction with Gd(III) is analyzed as described previously (*24*) in order to obtain the interspin distance, *r*, separating the two paramagnetic centers. The interspin distances (Table 1) confirm previous findings (*21*, *28*), although the distances estimated by this means appear to be greater than those obtained from either spin−spin interactions in the frozen state or thiol cross-linking (see *29*). Figure 4 shows the proposed helix packing arrangement of helices V, VII, and VIII which is consistent with the data of Wu et al. (*21*, *28*) and with the observations presented here.

The present data can be interpreted qualitatively only. Due to the many possible orientations the probes may assume with respect to the backbone, it is difficult to predict the direction and distance of the spin centers relative to the labeled side chain. Thus, it is unlikely that the distances reflect true distances separating the backbone attachment positions of the labeled Cys residues investigated here. The size of the Gd(III)−BAD compound and the length of the linker used are especially problematic. In this regard, distances estimated from Gd(III)−spin-label measurements are significantly greater than those estimated from spin−spin interactions between the same three pairs or from thiol cross-linking between Cys residues at positions 148 and 228 with dibromobimane, a rigid homobifunctional reagent about 5 Å in length (*21*, *28*). For example, analysis of the double-nitroxide I275R1/C148R1 mutant from (*21*, *28*) using a broadening function synthesized as a sum of Pake functions to represent a distance distribution (*20*) provides a good fit for an interspin distance of 17 Å (not shown). This compares

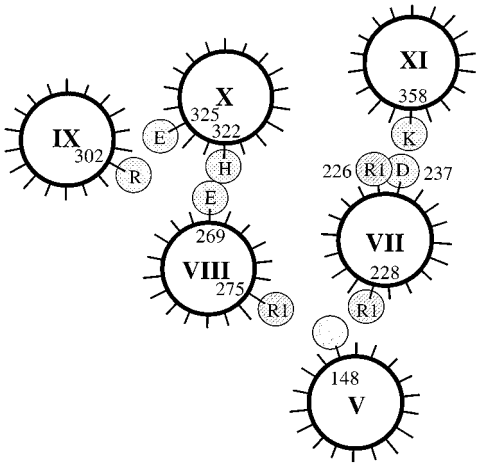

FIGURE 4: Arrangement of helices V, VII, and VIII in lac permease based on the data presented here and in Wu et al. (*21*). Helices are represented as circles with Roman numerals, and pertinent side chains are shown as shaded smaller circles. Cys148 (helix V) labeled with Gd(III)−BAD is lightly shaded; Cys residues at positions 275, 269 (helix VIII), or 228 (helix VII) are hatched and labeled as R1 (nitroxide spin-label). Charge pairs Arg302 (helix IX)/Glu325 (helix X), Glu269 (helix VIII)/His322 (helix X), and Asp237 (helix VII)/Lys358 (helix XI) are stippled (see *3*, *4*).

to a distance between the nitroxide and the Gd(III) chelator of 20 Å (Table 1), when the same sites are used. Thus, future prospects for this type of measurement would be enhanced with a more compact chelator, particularly one with a shortened linker. Quantitative interpretation of distance values should also be avoided due to uncertainty in the calculation arising from the value of T_{1e} (*24*). Here, $T_{1e} = 5.3 \times 10^{-10}$ is employed (*36*). However, since calculated distances depend on the sixth root of T_{1e}, the results are not critically dependent on an accurate value.

As shown previously (*24*), incorporation of a second paramagnetic center at a specific site in a protein has many advantages for the measurement of distances within proteins. The primary purpose for pursuing a metal−nitroxide approach with the Gd(III) chelator is the large magnetic moment of this ion ($8\mu_B$). Thus, theory suggests that detectable interaction with Gd(III) should extend about 10 Å beyond the range possible with Cu(II). Directing different probes to different residues with high specificity remains a challenge, and use of this approach with double-Cys mutants in other proteins may not be practical in general. Obviously, it is rare that the protein of interest contains a highly reactive residue that can be completely blocked by a diffusable reagent. The use of a single-Cys mutant combined with an engineered (or intrinsic) metal binding site, as described previously (*24*, *26*), overcomes this problem. Furthermore, lanthanides are known to bind with high affinity to intrinsic Ca(II) binding sites (EF hand motifs) (*38*, *39*). In addition, Ca(II) binding sites have been engineered into proteins (*40*−*43*), and such motifs would be particularly useful for introducing Gd(III).

In summary, development of double labeling approaches holds great promise for the study of protein structure and dynamics (*2*). An advantage of the technique is that it allows studies of a single engineered protein by both magnetic resonance and optical spectroscopy. An in vitro translation method using an amber supressor tRNA charged with an unnatural amino acid has been developed for this purpose

(*44*). By using this approach, Cornish et al. (*45*) have incorporated spectroscopic probes directly into T4 lysozyme. Other possibilities for directing unique probes to two sites include modifying an Arg-Cys pair (*46*) or specifically directing one probe to the amino terminus and a second to a single Cys residue. Finally, functional permease mutants devoid of Cys (*47*) or Trp (*48*) have been constructed. Insertion of an EF hand motif to bind rare earth metals into mutants containing single-Cys residues that can be labeled with nitroxides or fluorescent probes or single-Trp residues should significantly extend double labeling approaches with respect to SDSL, as well as fluorescence and luminescence energy transfer.

REFERENCES

1. Hyde, J. S., Swartz, H. M., and Antholine, W. E. (1979) in *Spin Labeling II* (Berliner, L. J., Ed.) pp 71−113, Academic Press, New York.
2. Likhtenshtein, G. I. (1993) *Biophysical labeling methods in molecular biology*, Cambridge University Press, New York.
3. Frillingos, S., Sahin-Tóth, M., Wu, J., and Kaback, H. R. (1998) *FASEB J. 12*, 1281−1299.
4. Kaback, H. R., and Wu, J. (1999) *Acc. Chem. Res. 32*, 805−813.
5. Wu, J., and Kaback, H. R. (1994) *Biochemistry 33*, 12166−12171.
6. Frillingos, S., and Kaback, H. R. (1996) *Biochemistry 35*, 3950−3956.
7. Sahin-Tóth, M., le Coutre, J., Kharabi, D., le Maire, G., Lee, J. C., and Kaback, H. R. (1999) *Biochemistry 38*, 813−819.
8. Sahin-Tóth, M., Akhoon, K. M., Runner, J., and Kaback, H. R. (2000) *Biochemistry 39*, 5907−5103.
9. Hubbell, W. L., and Altenbach, C. A. (1994) in *Membrane Protein Structure* (White, S. H., Ed.) pp 224−248, Oxford University Press, New York.
10. Todd, A. P., Cong, J., Levinthal, F., Levinthal, C., and Hubbell, W. L. (1989) *Proteins: Struct., Funct., Genet. 6*, 294−305.
11. Greenhalgh, D. A., Altenbach, C., Hubbell, W. L., and Khorana, H. G. (1991) *Proc. Natl. Acad. Sci. U.S.A. 88*, 8626−8630.
12. Altenbach, C., Greenhalgh, D. A., Khorana, H. G., and Hubbell, W. L. (1994) *Proc. Natl. Acad. Sci. U.S.A. 91*, 1667−1671.
13. Zhan, H., Oh, K. J., Shin, Y. K., Hubbell, W. L., and Collier, R. J. (1995) *Biochemistry 34*, 4856−4863.
14. Voss, J., He, M., Hubbell, W., and Kaback, H. R. (1996) *Biochemistry 35*, 12915−12918.
15. Voss, J., Hubbell, W. L., Hernandez, J., and Kaback, H. R. (1997) *Biochemistry 36*, 15055−15061.
16. Zhao, M., Zen, K.-C., Hernandez-Borrell, J., Altenbach, C., Hubbell, W. L., and Kaback, H. R. (1999) *Biochemistry 38*, 15970−15977.
17. Altenbach, C., Marti, T., Khorana, H. G., and Hubbell, W. L. (1990) *Science 248*, 1088−1092.
18. Mchaourab, H., Lietzow, M. A., Hideg, K., and Hubbell, W. L. (1996) *Biochemistry 35*, 7692−7704.
19. Steinhoff, H. J., Mollaaghababa, R., Altenbach, C., Hideg, K., Krebs, M., Khorana, H. G., and Hubbell, W. L. (1994) *Science 266*, 105−107.
20. Rabenstein, M. S., and Shin, Y.-K. (1995) *Proc. Natl. Acad. Sci. U.S.A. 92*, 8239−8243.
21. Wu, J., Voss, J., Hubbell, W. L., and Kaback, H. R. (1996) *Proc. Natl. Acad. Sci. U.S.A. 93*, 10123−10127.
22. Wang, Q., Voss, J., Hubbell, W. L., and Kaback, H. R. (1998) *Biochemistry 37*, 4910−4915.
23. Zhao, M., Zen, K.-C., Hubbell, W., and Kaback, H. R. (1999) *Biochemistry 38*, 7407−7412.
24. Voss, J., Salwinski, L., Kaback, H. R., and Hubbell, W. L. (1995) *Proc. Natl. Acad. Sci. U.S.A. 92*, 12295−12299.
25. Voss, J., Hubbell, W. L., and Kaback, H. R. (1995) *Proc. Natl. Acad. Sci. U.S.A. 92*, 12300−12303.
26. Voss, J., Hubbell, W. L., and Kaback, H. R. (1998) *Biochemistry 37*, 211−216.
27. Leigh, J. S. (1970) *J. Chem. Phys. 52*, 2608−2612.
28. Wu, J., Perrin, D., Sigman, D., and Kaback, H. (1995) *Proc. Natl. Acad. Sci. U.S.A. 92*, 9186−9190.
29. Sun, J., Voss, J., Hubbell, W. L., and Kaback, H. R. (1999) *Biochemistry 38*, 3100−3105.
30. Renn, O., and Meares, C. F. (1992) *Bioconjugate Chem. 3*, 563−569.
31. Moran, J. K., Greiner, D. P., and Meares, C. F. (1995) *Bioconjugate Chem. 6*, 296−301.
32. Kumar, K., Chang, C. A., Francesconi, L. C., Dischino, D. D., Malley, M. F., Gougoutas, J. Z., and Tweedle, M. F. (1994) *Inorg. Chem. 33*, 3567−3575.
33. Froncisz, W., and Hyde, J. S. (1982) *J. Magn. Reson. 47*, 515−521.
34. Hubbell, W. L., Froncisz, W., and Hyde, J. S. (1987) *Rev. Sci. Instrum. 58*, 1879−1886.
35. Pake, G. E. (1962) *Paramagnetic Resonance*, W. A. Benjamin, Inc., New York.
36. Dwek, R. A., Levy, H. R., Radda, G. K., and Seeley, P. J. (1975) *Biochim. Biophys. Acta 377*, 26−33.
37. Altenbach, C., Yang, K., Farrens, D., Khorana, H. G., and Hubbell, W. L. (1996) *Biochemistry 35*, 12470−12478.
38. Henao, F., Orlowski, S., Merah, Z., and Champeil, P. (1992) *J. Biol. Chem. 267*, 10302−10312.
39. Fernando, K. C., and Barrit, G. J. (1995) *Biochim. Biophys. Acta 1268*, 97−106.
40. Regan, L. (1993) *Annu. Rev. Biophys. Biomol. Struct. 22*, 257−287.
41. Kuroki, R., Taniyama, Y., Seko, C., Nakamura, H., Kikuchi, M., and Ikehara, M. (1989) *Proc. Natl. Acad. Sci. U.S.A. 86*, 6903−6907.
42. Toma, S., Campagnoli, S., Margarit, I., Gianna, R., Grandi, G., Bolognesi, M., De Filippis, V., and Fontana, A. (1991) *Biochemistry 30*, 97−106.
43. Clark, I. D., MacManus, J. P., Banville, D., and Szabo, A. G. (1993) *Anal. Biochem. 210*, 1−6.
44. Noren, C. J., Anthony-Cahill, S. J., Griffith, M. C., and Schultz, P. G. (1989) *Science 244*, 182−188.
45. Cornish, V. W., Benson, D. R., Altenbach, C. A., Hideg, K., Hubbell, W. L., and Schultz, P. G. (1994) *Proc. Natl. Acad. Sci. U.S.A. 91*, 2910−2914.
46. Hankovszky, H. O., Hideg, K., Goldammer, E. V., Matuszak, E., Kolkenbrock, H., Tschesche, H., and Wenzel, H. R. (1987) *Biochim. Biophys. Acta 916*, 152−155.
47. van Iwaarden, P. R., Pastore, J. C., Konings, W. N., and Kaback, H. R. (1991) *Biochemistry 30*, 9595−9600.
48. Menezes, M. E., Roepe, P. D., and Kaback, H. R. (1990) *Proc. Natl. Acad. Sci. U.S.A. 87*, 1638−1642.

BI002333E